

Fast quantum gate design with deep reinforcement learning using real-time feedback on readout signals

Emily Wright

*Department of Physics and Astronomy
University of Victoria
Victoria, Canada
emilywright1@uvic.ca*

Rogério de Sousa

*Department of Physics and Astronomy
University of Victoria
Victoria, Canada
rdesousa@uvic.ca*

Abstract—The design of high-fidelity quantum gates is difficult because it requires the optimization of two competing effects, namely maximizing gate speed and minimizing leakage out of the qubit subspace. We propose a deep reinforcement learning algorithm that uses two agents to address the speed and leakage challenges simultaneously. The first agent constructs the qubit in-phase control pulse using a policy learned from rewards that compensate short gate times. The rewards are obtained at intermediate time steps throughout the construction of a full-length pulse, allowing the agent to explore the landscape of shorter pulses. The second agent determines an out-of-phase pulse to target leakage. Both agents are trained on real-time data from noisy hardware, thus providing model-free gate design that adapts to unpredictable hardware noise. To reduce the effect of measurement classification errors, the agents are trained directly on the readout signal from probing the qubit. We present proof-of-concept experiments by designing X and square root of X gates of various durations on IBM hardware. After just 200 training iterations, our algorithm is able to construct novel control pulses up to two times faster than the default IBM gates, while matching their performance in terms of state fidelity and leakage rate. As the length of our custom control pulses increases, they begin to outperform the default gates. Improvements to the speed and fidelity of gate operations open the way for higher circuit depth in quantum simulation, quantum chemistry and other algorithms on near-term and future quantum devices.

Index Terms—Superconducting qubits, Optimal control, Reinforcement learning

I. INTRODUCTION

Hardware noise, fabrication variability, and imperfect logic gates are the greatest barriers to performing reliable quantum computations at a large-scale [1]. Presently, gate operations on quantum computers such as those produced by IBM are realized with derivative removal by adiabatic gate (DRAG) pulses calculated analytically from a simple three-level model [2]. The fidelity of these gate operations suffers due to long gate times, imperfect models, and time-dependent changes in the processor parameters such as qubit frequencies. Frequent calibration to combat these fluctuations is costly and even when properly calibrated, the control pulse shapes are sub-optimal and allow for errors. Decoherence and leakage out of the computational sub-space are of particular concern in the context of fault-tolerant quantum computing as they require substantial additional resources to correct and can significantly impact the threshold of certain error correction codes [3]–[6]. Thus, engineering faster and higher-fidelity gates is of timely importance.

Existing strategies for gateset design are analytic [2], [7]–[10] or based on numerical simulations that require precise physical and noise models of the hardware [11]–[17]. In large-scale quantum processors, the difficulty of completely characterizing the system prohibits model-based control techniques. Reinforcement learning (RL) [18]–[20] is an alternative approach for gate design which operates without prior knowledge of the hardware model. RL and its variants have been applied to myriad quantum control problems using numerically simulated environments [21]–[37]. Such set-ups demonstrate the potential of RL, but suffer from the same modelling constraints as other optimization methods. Recently, a few experiments have been carried out using RL directly on noisy hardware [38]–[41].

In this paper, we propose a new RL algorithm to design fast quantum gates. Our algorithm has several advantages over existing proposals including:

- 1) enabling design of faster gates by rewarding intermediate steps in the control pulse,
- 2) reducing the impact of measurement errors by training directly on the readout signal rather than classifying the state,

This work was supported by the Natural Sciences and Engineering Research Council of Canada (NSERC) through its Discovery (RGPIN-2020-04328), CREATE (543245-2020), and CGS M programs. Cette oeuvre a été soutenue par le Conseil de recherches en sciences naturelles et en génie du Canada (CRSNG) via ses programmes Discovery (RGPIN-2020-04328), CREATE (543245-2020) et CGS M.

- 3) mitigating leakage with a dual agent architecture,
- 4) speeding up training using low measurement overhead and real-time feedback, and
- 5) accounting for realistic noise in the quantum processor by training directly on hardware.

As well, we initialize the agent by pre-training on a calibrated DRAG pulse to capture information about the system dynamics. We optimize X and \sqrt{X} gates of different durations as a proof-of-concept; however, our algorithm can easily be extended to two-qubit gates by modifying the reward function and state space to complete a universal gateset.

The paper is structured as follows: in Section II we introduce the general RL algorithm, in Section III we review the related literature, in Section IV we describe our deep RL algorithm for fast quantum gate design, in Section V we present experimental results, and in Section VI we describe the extension of our algorithm to two-qubit gates.

II. THE RL ALGORITHM

In this section, we describe the RL algorithm in detail. RL is a machine learning algorithm wherein an agent interacts with a system and iteratively updates a control policy based on its observations. The entire process is modelled as a controlled Markov Decision Process (MDP). Let $\mathbb{S} \subset \mathbb{R}^n$ be the space of states for the system and \mathbb{U} the set of possible actions. At each step, the system is in some state s_j and the agent decides on an action u_j according to a policy. The policy $\pi(\cdot|s_j)$ is a conditional probability distribution over the possible actions in \mathbb{U} given the current state. The system moves into the next state s_{j+1} via a stochastic transition kernel $\mathcal{T}(\cdot|s_j, u_j)$. After observing the next state, the agent receives a corresponding reward $r_j(s_j, u_j, s_{j+1})$. The objective of the controller is to maximize the infinite-horizon discounted expected reward

$$J_\beta(s_0, \pi) = E_{s_0}^{\mathcal{T}, \pi} \left[\sum_{j=0}^{\infty} \beta^j r_j(s_j, u_j, s_{j+1}) \right] \quad (1)$$

over the set of admissible policies π , where $0 < \beta < 1$ is a discount factor and $E_{s_0}^{\mathcal{T}, \pi}$ denotes the expectation for initial state s_0 and transition kernel \mathcal{T} under policy π .

The standard RL algorithm is Q-learning [19]. Q-learning involves tracking the “value” of taking an action u_j given the current state s_j . The Q-value is stored in a table indexed by states and actions. Given an initial table Q_0 , the value of each state-action pair is updated according to the Bellman equation

$$Q_{j+1}(s_j, u_j) = Q_j(s_j, u_j) + \alpha_j(s_j, u_j) \left[r(s_j, u_j, s_{j+1}) + \beta \max_{v \in \mathbb{U}} Q_j(s_{j+1}, v) - Q_j(s_j, u_j) \right] \quad (2)$$

as the agent explores the environment [19]. The coefficient α_j is a hyperparameter called the learning rate and determines how quickly the agent adapts to changes in the environment. Under mild conditions on the learning rate, the algorithm converges to a fixed point denoted Q_* , which satisfies

$$Q_*(s, u) = E \left[r(s, u, s') + \beta \max_{v \in \mathbb{U}} Q_*(s', v) \mid s, u \right]. \quad (3)$$

A policy π which satisfies

$$\max_{u \in \mathbb{U}} Q_*(s, u) = Q_*(s, \pi(s)) \quad (4)$$

is an optimal policy (see Theorem 4 in [18] and the main Theorem in [19]).

The Q-learning algorithm was conceived for finite action and state spaces. For large and/or continuous state spaces, storing the Q-value in a table is not an option. To overcome this challenge, one might quantize the state space [42] or use function approximation [43]. While Q-learning with quantization or function approximation is not guaranteed to converge, there is ample empirical evidence that it can be used to solve quantum control problems [21]–[41]. In this work, we approximate the Q-table using a neural network, in a strategy that has been termed “deep reinforcement learning” (DRL) [44], [45]. The state s_j is the input to the neural network and the output is a probability distribution $\pi(\cdot|s_j)$ over the action space \mathbb{U} . The neural network is represented by a set of parameters θ which are updated in a manner that approximates the Bellman equation [46].

III. RL FOR QUANTUM GATE DESIGN

Having introduced RL, we now review its uses for quantum gate design to-date. Many RL algorithms have been proposed to solve quantum control problems in areas ranging from Hamiltonian engineering [23] to quantum metrology [22]. Theoretical algorithms make use of simulated environments to provide full access to the state of the quantum system [21]–[30]. Of these proposals, several specifically target unitary gate design [25], [47], [48]. In all cases, the agent has access to the exact unitary operator specifying the Schrödinger evolution of the system. In [25], [47] a simplified Hamiltonian model is used while [48] simulates a gmon environment which mimics noisy control actuation and incorporates leakage errors. The agents receive rewards based on gate infidelity which is inaccessible in experiments. In simulation, these algorithms are able to achieve improvements in gate fidelity [25], [47], [48] and gate time [25], [48] over other gate synthesis strategies. However, these proposals are not compatible with training on real hardware thus necessarily suffer from model bias. More realistic RL set-ups for quantum control only provide access to fidelities and/or expectation values for some observables [31]–[37]. Specifically for gate design, Shindi et al. proposed in [31] to probe a gate with a series of input states. The reward incorporates the average fidelity between the output states and the target states. Such algorithms require prohibitive amounts of averaging in experiments so they are also confined to numerical simulations.

The next step is to perform RL using stochastic measurement outcomes or low-sample estimators of physical observable [38]–[41]. Most recently, some experiments have been carried out using RL directly on noisy quantum hardware [38], [39]. Baum et al. trained a DRL agent on a superconducting computer for error-robust gateset design [39]. The agent was able to learn novel pulse shapes up to three times faster than industry standard DRAG gates with slightly lower error per gate

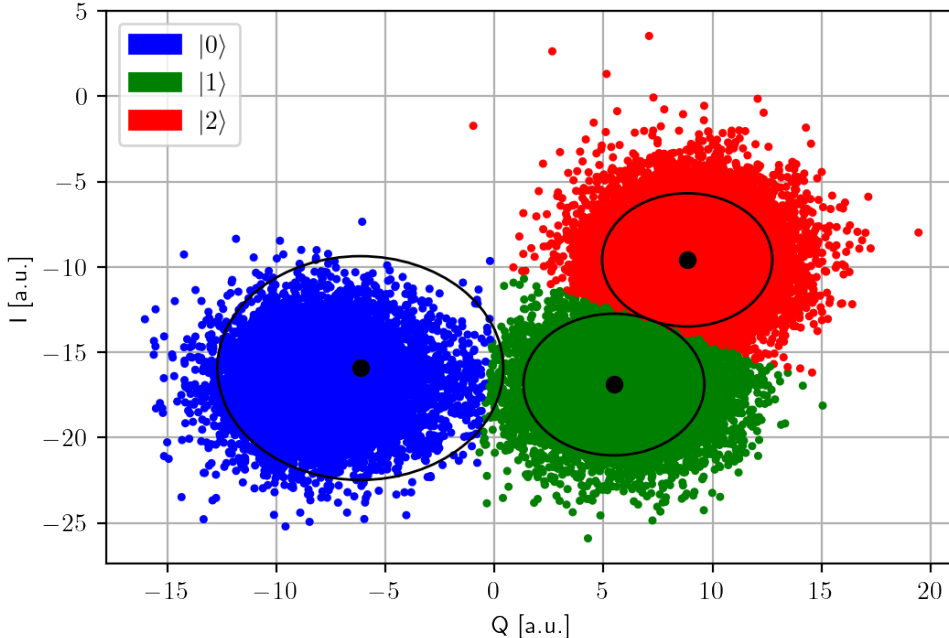


Figure 1: A plot of the readout signal for different qubit states (10000 shots each) on IBM Lima. Black circles indicate the mean and standard deviation of each cluster. The overlap shows the difficulty of distinguishing between states.

and improvements maintained without re-calibration for up to 25 days. The search space was restricted to 8 and 10 segment piece-wise constant operations for one- and two-qubit gates respectively. Despite the small search space, the optimization algorithm was inefficient. The training was completed in batches and the reward was a weighted mean over fidelities estimated using full state tomography. Subsequently, Reuer et al. developed a latency-based DRL agent implemented via an FPGA capable of using real-time feedback at the microsecond time scale [38]. They demonstrated its effectiveness with a state preparation experiment on a superconducting qubit. In this paper, we look ahead to a future where real-time feedback for quantum control is common. We improve upon the work in [39] by allowing greater flexibility in pulse shapes, training directly on the readout signal to reduce the impact of measurement errors, specifically targeting leakage errors, and relying on real-time feedback to speed-up the learning process.

IV. OUR DRL ALGORITHM FOR FAST QUANTUM GATE DESIGN

We now describe our DRL algorithm for design of fast quantum gates in detail. Here, we outline our algorithm specifically for superconducting transmon qubits, but it can easily be adapted to other hardware platforms such as trapped ions [49], quantum dots [50], or neutral atoms [51]. In this case, the quantum system consists of a transmon qubit dispersively coupled to a superconducting resonator and controlled via a capacitively coupled voltage drive line (see Appendix A for

details). The voltage drive envelope

$$c(t) = \begin{cases} c^x(t) \cos(\omega_d t) + c^y(t) \sin(\omega_d t) & 0 < t < t_g \\ 0 & \text{otherwise} \end{cases} \quad (5)$$

is composed of two independent quadrature controls $c^x(t)$ and $c^y(t)$ on a single drive frequency ω_d for the duration of the gate operation t_g . We seek to design a piece-wise constant (PWC) control pulse with up to N_{seg} segments of equal length $\tau = t_g/N_{\text{seg}}$ where t_g is the maximum duration of the gate.

Our DRL algorithm consists of two neural networks to decide sequentially on the x - and y -quadrature of the control pulse. The dual agent structure enables us to mitigate leakage errors while simultaneously creating faster gates. At each time step, our agents select the amplitudes of the next segment based on real-time feedback about the state of the system. The agents receive rewards throughout the construction of the pulse (rather than just at the end) which opens the possibility to design faster gates. We eliminate model-bias by training on quantum hardware so our DRL algorithm can account for realistic noise in the qubits and for other errors such as over-rotation introduced by the classical drive lines. We train directly on the observation signal resulting from probing the qubit. The signal has two components which we denote I for “in-phase” and Q for “quadrature”. Previous algorithms for gate design have used the $|0\rangle$ and $|1\rangle$ populations imperfectly estimated from the location of the signal in the (I, Q) -plane. Figure 1 shows readout data taken on the IBM Lima quantum computer, where there is overlap between the locations of the $|0\rangle$, $|1\rangle$, and $|2\rangle$ measurements. Our algorithm reduces the impact of measurement errors because we avoid classifying the

signal into $|0\rangle$ or $|1\rangle$. It also has a low measurement overhead since we do not perform full state tomography.

The network parameters θ^x, θ^y are updated periodically during the training. Each training iteration for $i = 0, \dots, N_{\text{iter}} - 1$ consists of $N_{\text{ep}} \leq N_{\text{seg}}$ episodes counted using the index j . The ratio $N_{\text{seg}}/N_{\text{ep}}$ is an integer that sets how many times the neural network parameters are updated before a full waveform is constructed. We use a second index $k = k(i, j)$ to track the waveform segment. The j -th input to the first neural network is a state $s_j^x = (\langle I_j \rangle, \langle Q_j \rangle, k)$ composed of the average (I, Q) signal over N_{shot} measurements and the current segment index k . The output of the agent is a probability distribution over the action space \mathbb{U}^x which we denote $\pi_{\theta_i^x}(\cdot | s_j^x)$ to indicate the dependence on the neural network parameters θ_i^x . The agent samples an action $u_j^x \in \mathbb{U}^x$ according to $\pi_{\theta_i^x}(\cdot | s_j^x)$. The state for the second agent $s_j^y = (u_j^x, \mathcal{L}_j)$ is formed of the amplitude u_j^x on the first quadrature and the leakage population

$$\mathcal{L}_j = |\langle 2 | U_{k+1} | 0 \rangle|^2 \quad (6)$$

estimated from the (I, Q) -plane, where U_{k+1} represents the operation of evolving the qubit by the first $k + 1$ segments of the waveform. The agent now samples an action $u_j^y \in \mathbb{U}^y$ according to the output $\pi_{\theta_i^y}(\cdot | s_j^y)$ of the second network. The k -th segment of the control pulse thus takes the form

$$c(t) = u_j^x \cos(\omega_d t) + u_j^y \sin(\omega_d t) \quad (7)$$

for $k\tau \leq t < (k + 1)\tau$. Based on hardware parameters, we restrict the x -quadrature amplitudes to the set $\mathbb{U}^x = \{0.00, 0.01, \dots, 0.19, 0.20\}$ and the y -quadrature amplitudes to $\mathbb{U}^y = \{-0.10, -0.09, \dots, 0.09, 0.10\}$.

To train the agent, we require a reward function for each network. Let $c_T = (\langle I_T \rangle, \langle Q_T \rangle) \pm \sigma_T$ be the expected average measurement result after applying the target gate to the ground state (calibrated experimentally). During training, we penalize the distance of the observed measurement signal from $(\langle I_T \rangle, \langle Q_T \rangle)$ which encapsulates both a failure to steer the qubit into the desired state and leakage into higher energy levels. We use the reward function

$$r_j^x(s_{j+1}^x, c_T) = \min \left\{ 1 - \lambda k, \frac{\sigma_T}{\|(\langle I_{j+1} \rangle, \langle Q_{j+1} \rangle) - (\langle I_T \rangle, \langle Q_T \rangle)\|} - \lambda k \right\} \quad (8)$$

to train the first network, where the term λk penalizes the length of the control pulse for some coefficient $\lambda \in \mathbb{R}$. For the second network, we compensate low leakage populations with the reward

$$r_j^y(s_{j+1}^y) = \max \{0, \mathcal{L}_{\text{max}} - \mathcal{L}_{j+1}\} \quad (9)$$

where \mathcal{L}_{max} sets a limit on the allowable leakage. A summary of our DRL algorithm is shown in Algorithm 1.

The initial state s_0^x and leakage population \mathcal{L}_0 are estimated by measuring the qubit before performing any gate operations. The initial policies $\pi_{\theta_0^x}, \pi_{\theta_0^y}$ are generated based on the industry standard DRAG gate by pre-training the agent. The DRAG pulse is Gaussian with a derivative component on the second

Algorithm 1 DRL for fast quantum gate design

Require: initial state s_0^x , leakage \mathcal{L}_0 , and parameters θ_0^x, θ_0^y

- 1: Set $k = 0$
- 2: **for** each iteration $i = 0, \dots, N_{\text{iter}} - 1$ **do**
- 3: **for** each episode $j = 0, \dots, N_{\text{ep}} - 1$ **do**
- 4: **if** $k = N_{\text{seg}}$ **then**
- 5: Re-initialize waveform $k = 0$
- 6: Re-initialize state $s_j^x = s_0^x$
- 7: Re-initialize leakage $\mathcal{L}_j = \mathcal{L}_0$
- 8: **end if**
- 9: Select next action u_j^x according to policy $\pi_{\theta_i^x}(\cdot | s_j^x)$
- 10: Set $s_j^y = (u_j^x, \mathcal{L}_j)$
- 11: Select next action u_j^y according to policy $\pi_{\theta_i^y}(\cdot | s_j^y)$
- 12: Evolve qubit by first $k + 1$ segments of waveform
- 13: Measure qubit N_{shot} times to get $(\langle I_{j+1} \rangle, \langle Q_{j+1} \rangle)$
- 14: Update $k \rightarrow k + 1$
- 15: Set $s_{j+1}^x = (\langle I_{j+1} \rangle, \langle Q_{j+1} \rangle, k)$
- 16: Calculate reward r_j^x
- 17: Estimate leakage population \mathcal{L}_{j+1}
- 18: Calculate reward r_j^y
- 19: Reset qubit to $|0\rangle$
- 20: **end for**
- 21: Send trajectory $(s_0^x, u_0^x, r_0^x, s_1^x, u_1^x, r_1^x, \dots, r_{N_{\text{ep}}-1}^x)$ to first network
- 22: Update neural network parameters $\theta_i^x \rightarrow \theta_{i+1}^x$
- 23: Send trajectory $(s_0^y, u_0^y, r_0^y, s_1^y, u_1^y, r_1^y, \dots, r_{N_{\text{ep}}-1}^y)$ to second network
- 24: Update neural network parameters $\theta_i^y \rightarrow \theta_{i+1}^y$
- 25: **end for**

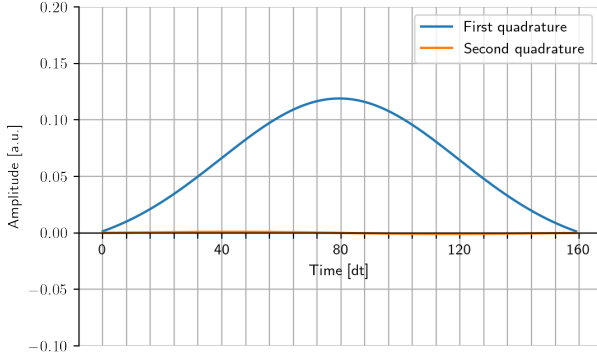
quadrature. That is, $c^x(t) = \Omega_G(t)$ and $c^y(t) = \gamma \Omega'_G(t)$ for a Gaussian envelope Ω_G and a coefficient $\gamma \in \mathbb{R}$ [2]. The DRAG pulse is designed to reduce leakage based on a simple three-level model. In experiments, the amplitude of Ω_G and the γ factor are calibrated to combat time dependent changes in the noise. Our initial policy captures information about the system dynamics using the calibrated DRAG pulse; however, our algorithm should not be considered an optimization of the DRAG pulse which has been proposed in other works [2], [52]. In the next section, we describe experimental results showing that our agent learns novel pulse shapes able to outperform the DRAG gate in terms of fidelity and leakage rate. For more details on the pre-training, see Appendix B.

V. EXPERIMENTAL RESULTS

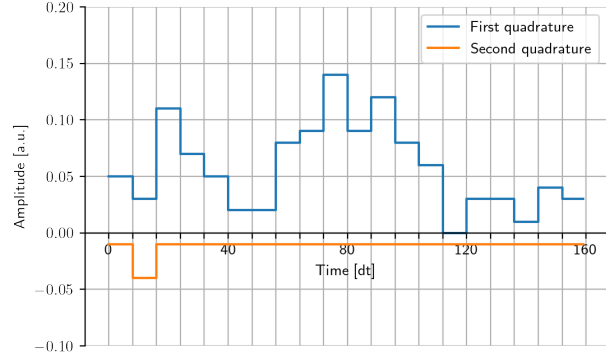
We conduct a proof-of-concept by designing the X and \sqrt{X} gates on the IBM Lima quantum computer using the Qiskit Pulse library [53], [54]. To assess the success of a gate U , we measure the leakage rate \mathcal{L} defined in (6) and the state fidelity

$$\mathcal{F} = |\langle \psi_T | U | 0 \rangle|^2 \quad (10)$$

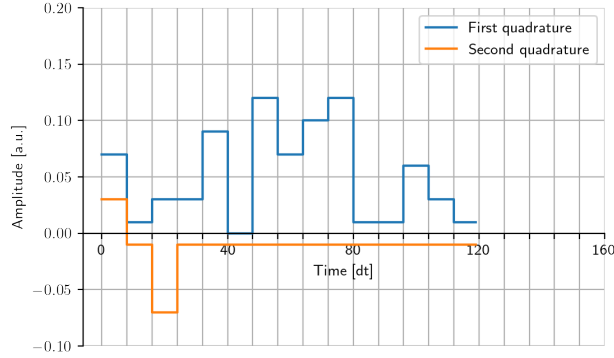
where $|\psi_T\rangle$ is the target state. We benchmark our fast quantum gates against DRAG gates, which are the industry standard used on many quantum computers including those produced



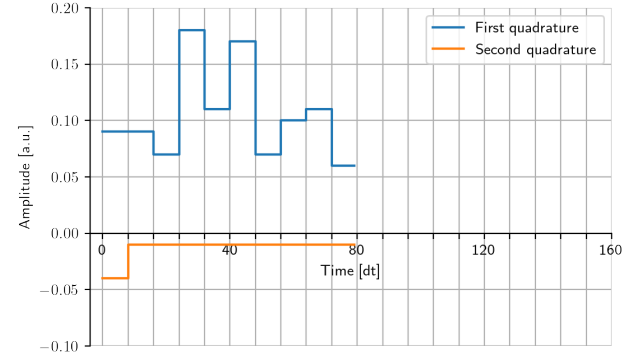
(a) DRAG X gate.



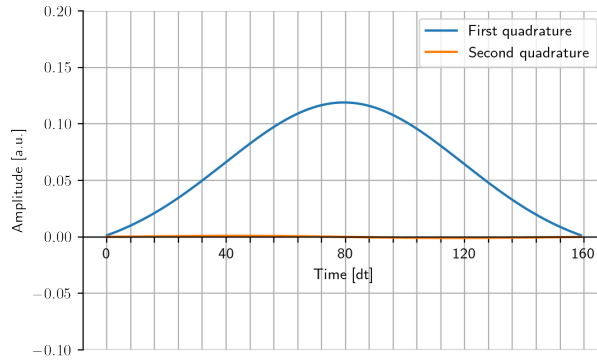
(b) Optimized X gate.



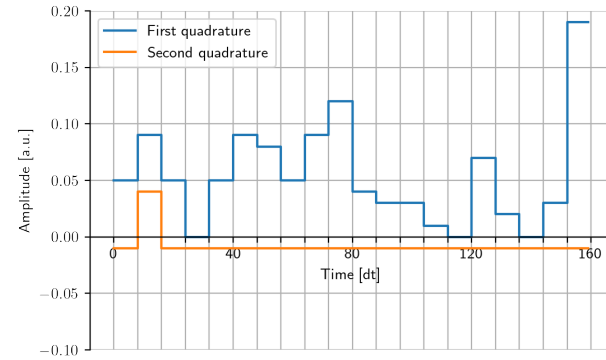
(c) Optimized X gate $1.33\times$ faster.



(d) Optimized X gate $2\times$ faster.



(e) DRAG X gate calibrated after 30 days.

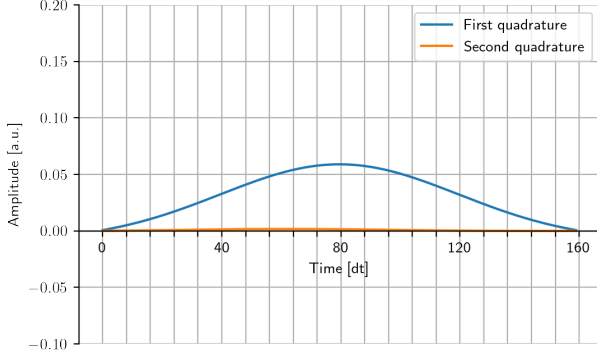
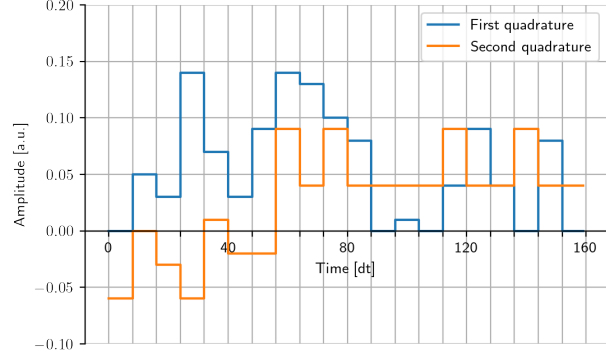
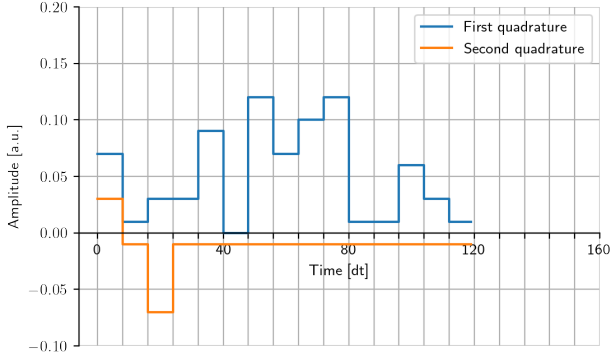
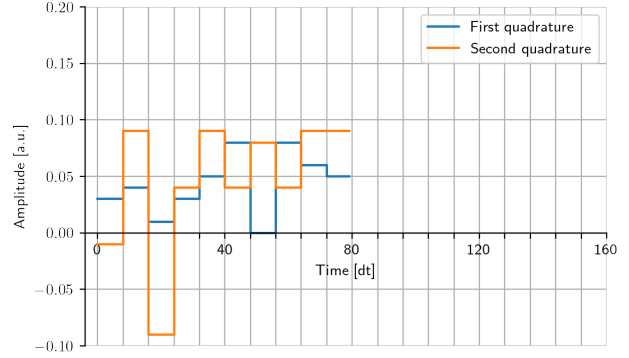


(f) Optimized X gate calibrated after 30 days.

Gate	Duration [ns]	Fidelity [%]	Leakage [%]
		(± 0.6)	(± 0.3)
DRAG X	35.6	91.7	4.2
Optimized X	35.6	92.2	3.5
Optimized X $1.33\times$ faster	26.7	92.2	4.3
Optimized X $2\times$ faster	17.8	90.4	3.8
DRAG X calibrated after 30 days	35.6	88.9	5.3
Optimized X calibrated after 30 days	35.6	89.2	4.3

(g) Summary of fidelities and leakage rates.

Figure 2: Plots showing default and optimized control pulses for single qubit gates on the IBM Lima quantum computer and their respective state fidelities and leakage rates. The time unit on the x -axis is in units of $dt = 0.222222$ ns, a device-dependent parameter specifying the maximum sampling rate of the waveform generator. Fig. (a) is a DRAG pulse for an X gate. Fig. (b) is a pulse for an X gate with duration 35.6 ns learned by our deep RL algorithm. Fig. (c) is a pulse for an X gate with duration 26.7 ns learned by our deep RL algorithm. Fig. (d) is a pulse for an X gate with duration 17.8 ns learned by our deep RL algorithm. Fig. (e) is a pulse for an X gate calibrated by our deep RL algorithm 30 days after training. Fig. (f) is a DRAG pulse for an X gate calibrated 30 days after training. Fig. (g) is table summarizing the state fidelities (10) and leakage rates (6) achieved by these gates.

(a) DRAG \sqrt{X} gate.(b) Optimized \sqrt{X} gate.(c) Optimized \sqrt{X} gate $1.33\times$ faster.(d) Optimized \sqrt{X} gate $2\times$ faster.

Gate	Duration [ns]	Fidelity [%] (± 0.6)	Leakage [%] (± 0.3)
DRAG \sqrt{X}	35.6	96.8	2.5
Optimized \sqrt{X}	35.6	97.5	2.4
Optimized \sqrt{X} $1.33\times$ faster	26.7	96.8	2.9
Optimized \sqrt{X} $2\times$ faster	17.8	96.5	3.5

(e) Summary of fidelities and leakage rates.

Figure 3: Plots showing default and optimized control pulses for single qubit gates on the IBM Lima quantum computer and their respective state fidelities and leakage rates. The time unit on the x -axis is in units of $dt = 0.222222$ ns, a device-dependent parameter specifying the maximum sampling rate of the waveform generator. Fig. (a) is a DRAG pulse for an \sqrt{X} gate. Fig. (b) is a pulse for an \sqrt{X} gate with duration 35.6 ns learned by our deep RL algorithm. Fig. (c) is a pulse for an \sqrt{X} gate with duration 26.7 ns learned by our deep RL algorithm. Fig. (d) is a pulse for an \sqrt{X} gate with duration 17.8 ns learned by our deep RL algorithm. Fig. (e) is table summarizing the state fidelities (10) and leakage rates (6) achieved by these gates.

by IBM. The trained agent can create gates of any number of segments from 1 to N_{seg} . We test gates of length 20 segments ($t_g \approx 35.6$ ns) – the same length as the DRAG gate –, 15 segments ($t_g \approx 26.7$ ns), and 10 segments ($t_g \approx 17.8$ ns). After just 200 training iterations, the faster gates begin to match the performance of the default gate, with fidelities and leakage rates the same or only slightly worse. Our full-length optimized gates begin to achieve higher state fidelities and lower leakage rates than the calibrated DRAG pulses. The optimized X and \sqrt{X} gates are shown in Figures 2 and 3

respectively alongside the corresponding DRAG pulses. The fidelities and leakage rates for each gate are summarized in Figures 2g and 3e.

We also test the robustness of our agent over time. Figure 2f shows a new optimized X gate created 30 days after the agent was trained. Again, it has slightly higher fidelity and lower leakage than the calibrated DRAG pulse. This shows that our agent does not require any additional training after 30 days. After an initial training period, our algorithm can be used to efficiently calibrate gates on superconducting qubits.

Due to limited access to hardware, we do not train our agent beyond 200 iterations nor do we optimize the learning rate, neural network structure, number of segments, or other hyperparameters. Our algorithm has not fully converged after the first 200 training iterations. We expect to achieve more significant advantage after optimizing the algorithm hyperparameters including using more training iterations.

VI. GENERALIZATION TO TWO-QUBIT GATES

A small modification to state space and reward function generalizes our algorithm to the design of two-qubit gates. In superconducting transmon qubits, two-qubit interactions are generated via a cross-resonance (CR) pulse (i.e. driving the control qubit at the resonant frequency of the target qubit) [55]. The CR pulse corresponds to the gate $Z \otimes X$, an X rotation on the target qubit with the direction dependent on the state of the control qubit. The industry standard CR gate is a rounded square pulse with Gaussian rise and a derivative-pulse correction on the second quadrature [56]. To avoid spurious cross-talk, a simultaneous cancellation tone is applied to the target qubit. Baum et al. used RL to design an improved CR gate which did not require this extra pulse [39]. We take the same strategy, so our agent can learn an improved CR pulse shape using the action spaces \mathbb{U}^x and \mathbb{U}^y from the single qubit case. The state $\tilde{s}_j^x = (\langle I_j^1 \rangle, \langle Q_j^1 \rangle, \langle I_j^2 \rangle, \langle Q_j^2 \rangle, k)$ contains the average readout signal from each qubit. We use the reward

$$\begin{aligned} \tilde{r}_j^x(\tilde{s}_{j+1}^x, c_T^1, c_T^2) = \\ \frac{1}{2} (r_j^x(\langle I_{j+1}^1 \rangle, \langle Q_{j+1}^1 \rangle, k, c_T^1) + r_j^x(\langle I_{j+1}^2 \rangle, \langle Q_{j+1}^2 \rangle, k, c_T^2)) \end{aligned} \quad (11)$$

where r_j^x is defined in (8) and c_T^1, c_T^2 are the expected measurement locations for the first and second qubit respectively. For the second control quadrature, the leakage population is summed over both qubits to give the same state and reward as the single qubit case. The CR gate completes a universal gateset $\{CR, R_Z(\theta), X, \sqrt{X}\}$ when combined with arbitrary virtual Z rotations [57] and the single qubit gates shown in our proof-of-concept.

VII. CONCLUSION

We have created a DRL algorithm for fast quantum gate design using real-time feedback based on the readout signal from noisy hardware. RL is model free, as opposed to other gate synthesis strategies which require precise models that cannot capture the stochastic dynamics of the qubit. Our dual-agent architecture allows us to target competing goals of decreasing leakage and creating faster gates to reduce decoherence. Our proposed algorithm reduces the impact of measurement classification errors by training directly on the readout signal from probing the qubit. The low measurement overhead means that our algorithm can be trained on hardware, rather than a numerical simulation.

We carried out a proof-of-concept with X and \sqrt{X} gates of different durations on IBM's hardware. Our agent proposed novel control pulses which are two times faster than industry standard DRAG gates and match their performance in terms of

fidelity and leakage after just 200 training iterations. Our agent also created gates of the same duration as DRAG which offer slight improvements in fidelity and leakage. We also showed that our trained agent is robust over time.

So far, we had limited access to hardware and only ran the algorithm with one specific set of hyperparameters. As is well known, the performance of RL is greatly improved with fine tuning of hyperparameters [58]. We expect optimization of the algorithm hyperparameters to lead to much more significant advantage.

Our proof-of-concept was carried out on transmon qubits; however, our proposed DRL algorithm is general and can be used on other quantum hardware with adjustments to the state and action spaces (e.g. photon counts and laser pulses for trapped ion quantum computing [49]). The improved gate operations created by our DRL algorithm for fast quantum gate design open the way for more extensive applications on near term and future quantum devices with reduced decoherence and leakage which cannot be fixed by most error correction algorithms.

APPENDIX A TRANSMON HARDWARE

We apply our deep RL algorithm for fast quantum gate design to a transmon qubit, formed of the lowest two energy levels in the quantized spectrum of a superconducting circuit [59]. The transmon qubit is controlled via a capacitively coupled drive line. Quantum circuit analysis leads to the transmon Hamiltonian [60]

$$\mathcal{H} = \omega_q a^\dagger a + \frac{\alpha}{2} a^\dagger a^\dagger a a - ic(t)(a^\dagger - a) \quad (12)$$

where a, a^\dagger are the creation and annihilation operators, ω_q is the qubit frequency, α is the anharmonicity and $c(t)$ is the voltage envelope introduced in (5).

The transmon qubit is dispersively coupled to a superconducting resonator for measurement. The qubit is probed with a microwave signal, which scatters off the resonator and gets amplified. The resultant observation is comprised of time traces of the in-phase I and quadrature Q components of the digitized signal. The state of the qubit can be inferred from the location of the signal in the (I, Q) -plane. On noisy hardware, the locations often overlap in the (I, Q) -plane and a decision maker such as a linear discriminant analyzer [61] is necessary to predict the state (see Figure 1).

APPENDIX B PRE-TRAINING

In this section, we describe pre-training our agent. First, we discretize a calibrated DRAG pulse into an N_{seg} PWC pulse where the amplitude of each segment is the nearest action from \mathbb{U}^x and \mathbb{U}^y for the first and second quadratures respectively. For each k , we measure the average $(\langle I \rangle, \langle Q \rangle)$ signal and leakage \mathcal{L} after the first $k + 1$ segments of the waveform. Each agent receives a reward based on the mean squared error (MSE) between the policy output by the neural network given the input state and a Gaussian distribution over

the respective action space centered at the desired amplitude. The pre-training is performed for several iterations over the full pulse. The pre-training can be executed efficiently because the rewards and actions are not based on the state of the system so the circuits can all be run before updating the network parameters. At the end of the pre-training, the agents favour a DRAG pulse. While the agents subsequently learn novel pulse shapes, the exploration begins in a near-optimal region of the solution space.

REFERENCES

- [1] J. Preskill, “Quantum computing in the NISQ era and beyond,” *Quantum*, vol. 2, p. 79, Aug. 2018. [Online]. Available: <https://doi.org/10.22331/q-2018-08-06-79>
- [2] F. Motzoi, J. M. Gambetta, P. Rebentrost, and F. K. Wilhelm, “Simple pulses for elimination of leakage in weakly nonlinear qubits,” *Physical Review Letters*, vol. 103, p. 110501, Sep 2009. [Online]. Available: <https://link.aps.org/doi/10.1103/PhysRevLett.103.110501>
- [3] M. McEwen, D. Kafri *et al.*, “Removing leakage-induced correlated errors in superconducting quantum error correction,” *Nature Communications*, vol. 12, no. 1, p. 1761, 2021. [Online]. Available: <https://www.nature.com/articles/s41467-021-21982-y>
- [4] C. J. Wood and J. M. Gambetta, “Quantification and characterization of leakage errors,” *Physical Review A*, vol. 97, p. 032306, Mar 2018. [Online]. Available: <https://link.aps.org/doi/10.1103/PhysRevA.97.032306>
- [5] M. Suchara, A. W. Cross, and J. M. Gambetta, “Leakage suppression in the toric code,” *arXiv*, 2014. [Online]. Available: <https://arxiv.org/abs/1410.8562>
- [6] A. G. Fowler, “Coping with qubit leakage in topological codes,” *Physical Review A*, vol. 88, p. 042308, Oct 2013. [Online]. Available: <https://link.aps.org/doi/10.1103/PhysRevA.88.042308>
- [7] N. Khaneja, R. Brockett, and S. J. Glaser, “Time optimal control in spin systems,” *Physical Review A*, vol. 63, p. 032308, Feb 2001. [Online]. Available: <https://link.aps.org/doi/10.1103/PhysRevA.63.032308>
- [8] U. Boscain, G. Charlot, J.-P. Gauthier, S. Guérin, and H.-R. Jauslin, “Optimal Control in laser-induced population transfer for two- or three-level quantum systems,” *Journal of Mathematical Physics*, vol. 43, no. 5, pp. pp 2107–2132, May 2002. [Online]. Available: <https://hal.science/hal-00383019>
- [9] A. Pechen, N. Il’in, F. Shuang, and H. Rabitz, “Quantum control by von neumann measurements,” *Physical Review A*, vol. 74, p. 052102, Nov 2006. [Online]. Available: <https://link.aps.org/doi/10.1103/PhysRevA.74.052102>
- [10] S. Montangero, T. Calarco, and R. Fazio, “Robust optimal quantum gates for josephson charge qubits,” *Physical Review Letters*, vol. 99, no. 17, Oct 2007. [Online]. Available: <https://doi.org/10.1103/2Fphysrevlett.99.170501>
- [11] V. F. Krotov, *Global Methods in Optimal Control Theory*. Boston, MA: Birkhäuser Boston, 1993, pp. 74–121.
- [12] N. B. Dehaghani and F. L. Pereira, “High fidelity quantum state transfer by pontryagin maximum principle,” 2022. [Online]. Available: <https://arxiv.org/abs/2203.04361>
- [13] W. Zhu and H. Rabitz, “A rapid monotonically convergent iteration algorithm for quantum optimal control over the expectation value of a positive definite operator,” *The Journal of Chemical Physics*, vol. 109, no. 2, pp. 385–391, 1998. [Online]. Available: <https://pubs.aip.org/aip/jcp/article/109/2/385/476865>
- [14] D. D’Alessandro and M. Dahleh, “Optimal control of two-level quantum systems,” *IEEE Transactions on Automatic Control*, vol. 46, no. 6, pp. 866–876, 2001. [Online]. Available: <https://ieeexplore.ieee.org/document/928587>
- [15] N. Khaneja, T. Reiss, C. Kehlet, T. Schulte-Herbrüggen, and S. J. Glaser, “Optimal control of coupled spin dynamics: design of nmr pulse sequences by gradient ascent algorithms,” *Journal of Magnetic Resonance*, vol. 172, no. 2, pp. 296–305, 2005. [Online]. Available: <https://www.sciencedirect.com/science/article/abs/pii/S1090780704003696>
- [16] S. Machnes, E. Assémat, D. Tannor, and F. K. Wilhelm, “Tunable, flexible, and efficient optimization of control pulses for practical qubits,” *Physical Review Letters*, vol. 120, p. 150401, Apr 2018. [Online]. Available: <https://link.aps.org/doi/10.1103/PhysRevLett.120.150401>
- [17] P. Doria, T. Calarco, and S. Montangero, “Optimal control technique for many-body quantum dynamics,” *Physical Review Letters*, vol. 106, no. 19, May 2011. [Online]. Available: <https://doi.org/10.1103/2Fphysrevlett.106.190501>
- [18] J. N. Tsitsiklis, “Asynchronous stochastic approximation and q-learning,” *Machine Learning*, vol. 16, no. 3, pp. 185–202, 1994. [Online]. Available: <https://link.springer.com/article/10.1023/A:1022689125041>
- [19] C. Watkins and P. Dayan, “Q-learning,” *Machine Learning*, vol. 8, no. 3, pp. 279–292, Jul 1992. [Online]. Available: <https://link.springer.com/article/10.1007/BF00992698>
- [20] C. Szepesvari and M. L. Littman, “A unified analysis of value-function-based reinforcement-learning algorithms,” *Neural Computation*, vol. 11, pp. 2017–2060, 1999. [Online]. Available: <https://pubmed.ncbi.nlm.nih.gov/10578043/>
- [21] F. Metz and M. Bukov, “Self-correcting quantum many-body control using reinforcement learning with tensor networks,” 2022. [Online]. Available: <https://arxiv.org/abs/2201.11790>
- [22] Y. Qiu, M. Zhuang, J. Huang, and C. Lee, “Efficient and robust entanglement generation with deep reinforcement learning for quantum metrology,” *New Journal of Physics*, vol. 24, no. 8, p. 083011, aug 2022. [Online]. Available: <https://doi.org/10.1088/2F1367-2630/2Fac8285>
- [23] P. Peng, X. Huang, C. Yin, L. Joseph, C. Ramanathan, and P. Cappellaro, “Deep reinforcement learning for quantum hamiltonian engineering,” 2021. [Online]. Available: <https://arxiv.org/abs/2102.13161>
- [24] Z. An, H.-J. Song, Q.-K. He, and D. L. Zhou, “Quantum optimal control of multilevel dissipative quantum systems with reinforcement learning,” *Physical Review A*, vol. 103, p. 012404, Jan 2021. [Online]. Available: <https://link.aps.org/doi/10.1103/PhysRevA.103.012404>
- [25] S. Daraeizadeh, S. P. Premaratne, and A. Y. Matsuura, “Designing high-fidelity multi-qubit gates for semiconductor quantum dots through deep reinforcement learning,” in *2020 IEEE International Conference on Quantum Computing and Engineering (QCE)*. IEEE, oct 2020. [Online]. Available: <https://doi.org/10.1109/2Fqce49297.2020.00014>
- [26] H. Ma, D. Dong, S. X. Ding, and C. Chen, “Curriculum-based deep reinforcement learning for quantum control,” 2020. [Online]. Available: <https://arxiv.org/abs/2012.15427>
- [27] J.-J. Chen and M. Xue, “Manipulation of spin dynamics by deep reinforcement learning agent,” 2019. [Online]. Available: <https://arxiv.org/abs/1901.08748>
- [28] R. Porotti, D. Tamascelli, M. Restelli, and E. Prati, “Coherent transport of quantum states by deep reinforcement learning,” *Communications Physics*, vol. 2, no. 1, jun 2019. [Online]. Available: <https://doi.org/10.1038/2F42005-019-0169-x>
- [29] X.-M. Zhang, Z. Wei, R. Asad, X.-C. Yang, and X. Wang, “When does reinforcement learning stand out in quantum control? a comparative study on state preparation,” *npj Quantum Information*, vol. 5, Oct 2019. [Online]. Available: <https://www.nature.com/articles/s41534-019-0201-8#citeas>
- [30] C. Chen, D. Dong, H.-X. Li, J. Chu, and T.-J. Tarn, “Fidelity-based probabilistic q-learning for control of quantum systems,” *IEEE Transactions on Neural Networks and Learning Systems*, vol. 25, no. 5, pp. 920–933, may 2014. [Online]. Available: <https://doi.org/10.1109/2Ftnnls.2013.2283574>
- [31] O. Shindi, Q. Yu, P. Girdhar, and D. Dong, “Model-free quantum gate design and calibration using deep reinforcement learning,” *arXiv*, 2023. [Online]. Available: <https://arxiv.org/abs/2302.02371>
- [32] V. V. Sivak, A. Eickbusch, H. Liu, B. Royer, I. Tsioutsios, and M. H. Devoret, “Model-free quantum control with reinforcement learning,” *Physical Review X*, vol. 12, p. 011059, Mar 2022. [Online]. Available: <https://link.aps.org/doi/10.1103/PhysRevX.12.011059>
- [33] S.-F. Guo, F. Chen *et al.*, “Faster state preparation across quantum phase transition assisted by reinforcement learning,” *Physical Review Letters*, vol. 126, no. 6, feb 2021. [Online]. Available: <https://doi.org/10.1103/2Fphysrevlett.126.060401>
- [34] E.-J. Kuo, Y.-L. L. Fang, and S. Y.-C. Chen, “Quantum architecture search via deep reinforcement learning,” *arXiv*, 2021. [Online]. Available: <https://arxiv.org/abs/2104.07715>
- [35] M. M. Wauters, E. Panizon, G. B. Mbeng, and G. E. Santoro, “Reinforcement-learning-assisted quantum optimization,” *Physical*

- Review Res.*, vol. 2, p. 033446, Sep 2020. [Online]. Available: <https://link.aps.org/doi/10.1103/PhysRevResearch.2.033446>
- [36] A. García-Sáez and J. Riu, “Quantum observables for continuous control of the quantum approximate optimization algorithm via reinforcement learning,” *arXiv*, vol. abs/1911.09682, 2019. [Online]. Available: <https://arxiv.org/abs/1911.09682>
- [37] M. Bukov, A. G. R. Day, D. Sels, P. Weinberg, A. Polkovnikov, and P. Mehta, “Reinforcement learning in different phases of quantum control,” *Physical Review X*, vol. 8, p. 031086, Sep 2018. [Online]. Available: <https://link.aps.org/doi/10.1103/PhysRevX.8.031086>
- [38] K. Reuer, J. Landgraf *et al.*, “Realizing a deep reinforcement learning agent discovering real-time feedback control strategies for a quantum system,” 2022. [Online]. Available: <https://arxiv.org/abs/2210.16715>
- [39] Y. Baum, M. Amico *et al.*, “Experimental deep reinforcement learning for error-robust gate-set design on a superconducting quantum computer,” *PRX Quantum*, vol. 2, no. 4, Nov 2021. [Online]. Available: <https://doi.org/10.1103/2Fprxquantum.2.040324>
- [40] S. Borah, B. Sarma, M. Kewming, G. J. Milburn, and J. Twamley, “Measurement-based feedback quantum control with deep reinforcement learning for a double-well nonlinear potential,” *Physical Review Letters*, vol. 127, p. 190403, Nov 2021. [Online]. Available: <https://link.aps.org/doi/10.1103/PhysRevLett.127.190403>
- [41] M. Bukov, “Reinforcement learning for autonomous preparation of floquet-engineered states: Inverting the quantum kapitza oscillator,” *Physical Review B*, vol. 98, no. 22, dec 2018. [Online]. Available: <https://doi.org/10.1103/2Fphysrevb.98.224305>
- [42] R. Gray and D. Neuhoff, “Quantization,” *IEEE Transactions on Information Theory*, vol. 44, no. 6, pp. 2325–2383, 1998.
- [43] A. Gadjiev and A. Ghorbanalizadeh, “Approximation of analytical functions by sequences of k-positive linear operators,” *Journal of Approximation Theory*, vol. 162, no. 6, pp. 1245–1255, 2010. [Online]. Available: <https://www.sciencedirect.com/science/article/pii/S0021904510000249>
- [44] D. Bertsekas and J. N. Tsitsiklis, *Neuro-dynamic programming*. Athena Scientific, 1996.
- [45] Y. Li, “Deep reinforcement learning: An overview,” *arXiv*, 2018. [Online]. Available: <https://arxiv.org/abs/1701.07274>
- [46] R. J. Williams, “Simple statistical gradient-following algorithms for connectionist reinforcement learning,” *Machine Learning*, vol. 8, no. 3, pp. 229–256, 1992. [Online]. Available: <https://link.springer.com/article/10.1007/BF00992696>
- [47] Z. An and D. L. Zhou, “Deep reinforcement learning for quantum gate control,” *EPL (Europhysics Letters)*, vol. 126, no. 6, p. 60002, Jul 2019. [Online]. Available: <https://doi.org/10.1209/2F0295-5075/2F126/2F60002>
- [48] M. Y. Niu, S. Boixo, V. N. Smelyanskiy, and H. Neven, “Universal quantum control through deep reinforcement learning,” *NPJ Quantum Information*, vol. 5, p. 33, Apr 2019. [Online]. Available: <https://www.nature.com/articles/s41534-019-0141-3#Bib1>
- [49] C. D. Bruzewicz, J. Chiaverini, R. McConnell, and J. M. Sage, “Trapped-ion quantum computing: Progress and challenges,” *Applied Physics Reviews*, vol. 6, no. 2, p. 021314, 2019. [Online]. Available: <https://doi.org/10.1063/2F1.5088164>
- [50] L. M. K. Vandersypen and M. A. Eriksson, “Quantum computing with semiconductor spins,” *Physics Today*, vol. 72, no. 8, pp. 38–45, 2019. [Online]. Available: <https://doi.org/10.1063/PT.3.4270>
- [51] L. Henriot, L. Beguin *et al.*, “Quantum computing with neutral atoms,” *Quantum*, vol. 4, p. 327, 2020. [Online]. Available: <https://doi.org/10.22331/2Fq-2020-09-21-327>
- [52] M. Werninghaus, D. J. Egger, F. Roy, S. Machnes, F. K. Wilhelm, and S. Filipp, “Leakage reduction in fast superconducting qubit gates via optimal control,” *npj Quantum Information*, vol. 7, no. 1, Jan 2021. [Online]. Available: <https://doi.org/10.1038/2Fs41534-020-00346-2>
- [53] Qiskit contributors, “Qiskit: An open-source framework for quantum computing,” 2023. [Online]. Available: <https://qiskit.org/>
- [54] D. C. McKay, T. Alexander *et al.*, “Qiskit backend specifications for openqasm and openpulse experiments,” *arXiv*, 2018. [Online]. Available: <https://arxiv.org/abs/1809.03452>
- [55] G. S. Paraoanu, “Microwave-induced coupling of superconducting qubits,” *Physical Review B*, vol. 74, p. 140504, Oct 2006. [Online]. Available: <https://link.aps.org/doi/10.1103/PhysRevB.74.140504>
- [56] S. Sheldon, E. Magesan, J. M. Chow, and J. M. Gambetta, “Procedure for systematically tuning up cross-talk in the cross-resonance gate,” *Physical Review A*, vol. 93, p. 060302, Jun 2016. [Online]. Available: <https://link.aps.org/doi/10.1103/PhysRevA.93.060302>
- [57] D. C. McKay, C. J. Wood, S. Sheldon, J. M. Chow, and J. M. Gambetta, “Efficient z gates for quantum computing,” *Physical Review A*, vol. 96, p. 022330, Aug 2017. [Online]. Available: <https://link.aps.org/doi/10.1103/PhysRevA.96.022330>
- [58] M. Feurer and F. Hutter, *Hyperparameter Optimization*. Cham: Springer International Publishing, 2019, pp. 3–33.
- [59] J. Koch, T. M. Yu *et al.*, “Charge-insensitive qubit design derived from the cooper pair box,” *Physical Review A*, vol. 76, no. 4, Oct 2007. [Online]. Available: <https://doi.org/10.1103/2Fphysrev.76.042319>
- [60] P. Krantz, M. Kjaergaard, F. Yan, T. P. Orlando, S. Gustavsson, and W. D. Oliver, “A quantum engineer’s guide to superconducting qubits,” *Applied Physics Reviews*, vol. 6, no. 2, p. 021318, jun 2019. [Online]. Available: <https://doi.org/10.1063/2F1.5089550>
- [61] E. Magesan, J. M. Gambetta, A. D. Córcoles, and J. M. Chow, “Machine learning for discriminating quantum measurement trajectories and improving readout,” *Physical Review Letters*, vol. 114, p. 200501, May 2015. [Online]. Available: <https://link.aps.org/doi/10.1103/PhysRevLett.114.200501>